Research Article

Defect Study of MgO-CaO Material Doped with CeO$_2$

Han Zhang, Huizhong Zhao, Jinfeng Chen, Jingjie Li, Jun Yu, and Jianhua Nie

The Hubei Province Key Laboratory of Ceramics and Refractories, Wuhan University of Science and Technology, 947 Heping Road, Wuhan 430081, China

Correspondence should be addressed to Han Zhang; wustzh@163.com

MgO-CaO refractories were prepared using analytical reagent chemicals of Ca(OH)$_2$ and Mg(OH)$_2$ as starting materials and CeO$_2$ as dopant, then sintered at 1650°C for 3 h. The effect of CeO$_2$ powders on the defect of MgO-CaO refractories was investigated. The sample characterizations were analyzed by the techniques of XRD and SEM. According to the results, with the addition of CeO$_2$, the lattice constant of CaO increased, and the bulk density of the samples increased while apparent porosity decreased. The densification of MgO-CaO refractories was promoted obviously. In the sintering process, MgO grains grew faster than CaO, pores at the MgO-CaO grain boundaries decreased while pores in the MgO grains increased gradually, and no pores were observed in the CaO grains. The nature of the CeO$_2$ promoting densification lies in the substitution and solution with CaO. Ce^{4+} approaches into CaO lattices, which enlarges the vacancy concentration of Ca^{2+} and accelerates the diffusion of Ca^{2+}.

1. Introduction

MgO-CaO refractories have been widely used in metallurgy industry [1] and cement rotary kilns [2] owing to their excellent properties such as high melting points, excellent thermal shock resistance, and slag corrosion resistance [3]. They have also been considered as one type of chrome-free refractories that are suitable for substituting the MgO-Cr$_2$O$_3$ refractories [4]. Furthermore, MgO-CaO refractories are beneficial to removing inclusions from molten steels; thus, they have been considered to be one of the effective refractory types for processing clean steel products [5, 6]. In recent years, with the increasing demands of molten steel purity, the awareness of environmental protection and resource shortage grows [7], and MgO-CaO materials have become one of the attractive steelmaking refractories because of their low cost and high ore reserves [8].

However, the application of MgO-CaO refractories has been limited by their poor hydration resistance [9, 10]. MgO-CaO materials are susceptible to hydration because the free lime in them can react easily with water, volume expansion of the resultant can cause severe damage to the materials.

The hydration resistance of free lime materials can be improved by treating them in a CO$_2$ atmosphere [11] which leads to the formation of a dense maskant on the surface of CaO. Further improvement may be made by adding metal oxides such as CuO [12], Fe$_2$O$_3$ [13], and SiO$_2$ [14] to react with lime to form a low-melting point phase or by adding ZrO$_2$ [15–17] to form high-melting stable compounds with CaO. However, the improvements made by using these methods are at the expense of reducing the free lime content, which deteriorates the high-temperature property of MgO-CaO refractories. It has been reported that the addition of rare earth oxides can appreciably improve the properties of the MgO-CaO refractories. However, the mechanisms for the improvements, especially the role played in the improvements by the lattice defects generated as a result of the doping of this type of oxides have not been adequately understood. In the present work, the effect of CeO$_2$ addition on the sintering and microstructure of the MgO-CaO refractories are investigated with an aim to delineate the effects of the lattice defects on improving the sintering and hydration resistance of MgO-CaO refractories.

2. Experimental Procedures

2.1. Raw Materials. In all the experiments, analytical reagent chemicals of Mg(OH)$_2$, Ca(OH)$_2$, and CeO$_2$ are used as raw materials. Powders of appropriate amounts of Mg(OH)$_2$ and

$Ca(OH)_2$ were weighed ($m_{MgO} : m_{CaO} = 8 : 2$) into a ceramic pot, then mixed in a planetary ball mill for 2 h at a speed of 180 r/min; the ball-to-powder weight ratio used was 3 : 1. The mixtures obtained were then light-roasted in a muffle furnace at 800°C for 30 min to obtain the MgO-CaO powders. 0-1 wt% of the CeO_2 powder was then dry-mixed with the light-roasted MgO-CaO powder. The mixture was then pressed to cylindrical samples of 20 mm in diameter and 20 mm in length under a pressure of 150 MPa. The samples were heated in an electric furnace at a rate of 3°C/min to 1650°C and kept for 3 h, followed by cooling to room temperature in the furnace.

2.2. Characterization of MgO-CaO Materials. The sintered samples were characterized by bulk density and apparent porosity measurements, microstructure, and phase composition analyses. The bulk density and apparent porosity were measured by Archimedes' principle using kerosene as an immersion medium under vacuum. The microstructure was analyzed by scanning electron microscopy (SEM, 20 kv). Phase compositions were determined by X-Ray powder diffraction (XRD, Cu target, 40 kv and 40 mA).

3. Results and Discussion

3.1. Densification. Figure 1 shows the effect of CeO_2 addition on bulk density and apparent porosity of the samples sintered at 1650°C for 3 h. It is observed that the bulk density increased gradually and the apparent porosity decreased with the addition of CeO_2. The bulk density increased to 3.35 g/cm^3 when the amount of CeO_2 added increased to 0.75 wt%. With further addition of CeO_2, however, the bulk density slightly decreased. These results indicate that adding small amounts of CeO_2 promoted the sintering and densification of MgO-CaO materials, but this enhancing effect reaches a maximum and starts to decrease when the amount of CeO_2 exceeds a certain level.

3.2. XRD Analysis. Figure 2 shows the XRD patterns of samples with and without CeO_2 additions. Periclase and lime were the main crystalline phases in all the samples. However, the intensity of diffraction peaks was higher for the samples with CeO_2 additions than for the sample without CeO_2 addition, indicating that CeO_2 promoted the growth of MgO and CaO grains, especially for the sample with 0.5 wt% CeO_2 added. The position of the diffraction peaks attributable to the CaO (2 2 2) crystallographic was shifted as a result of adding CeO_2, suggesting that Ce^{4+} entered into the CaO lattice, changing the lattice parameter of CaO. However, no apparent change in the positions of MgO diffraction peaks was detected.

The CaO lattice constant of the samples was determined (Table 1) by comparing the peak positions (2θ) of the XRD patterns using the least square method.

The lattice constant of CaO in the samples without CeO_2 addition was found to be 4.7978 Å, which was in accordance with the lattice constants of pure CaO. Adding CeO_2 increased the lattice constant of CaO. When the amount of
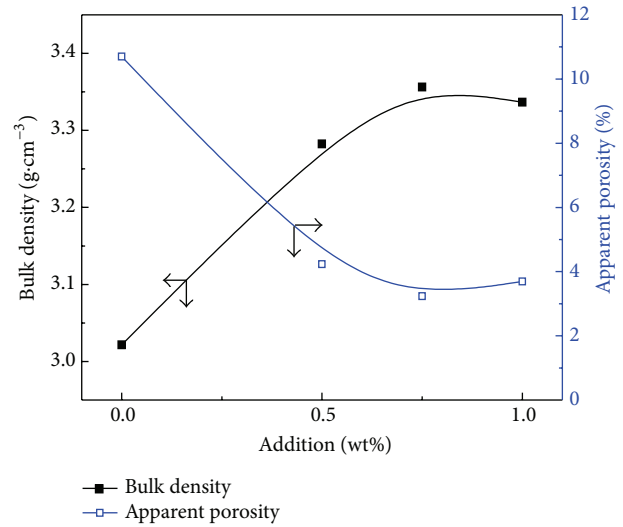

FIGURE 1: Effect of CeO_2 addition on bulk density and apparent porosity of samples.
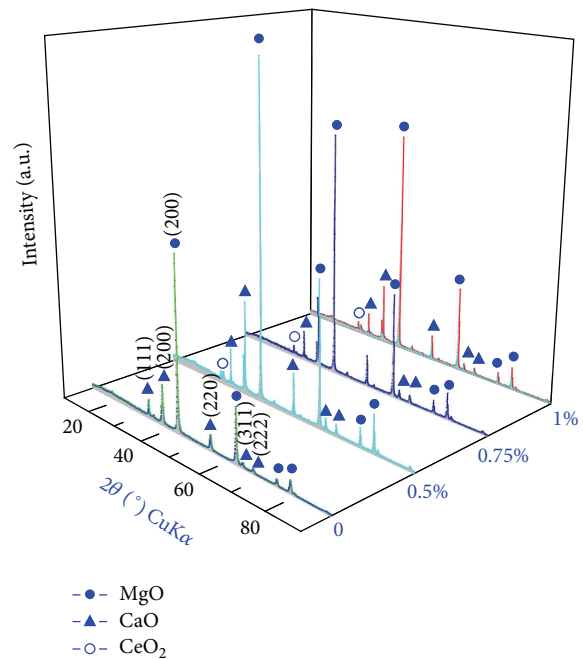

FIGURE 2: XRD patterns of pure and doped MgO-CaO samples.

CeO_2 added was 0.5 wt%, the lattice constant of CaO reached the highest point at $a_{CaO} = 4.8232$ Å. The lattice constants of CaO decreased with the further increase in CeO_2 content, but they were never below the value of the samples without CeO_2 addition.

Generally, the solid solution of metal oxides forms mainly by the replacement of positive ions in the solvent. Radius of positive ions directly affects the binding energy of positive and negative ions in ionic crystals and hence influences the solid solubility. When the difference in the radius of positive ions is less than 15%, it is easy to form a solid solution; when the difference is larger than 30%, it is not possible to form a

Table 1: Calculated lattice constant for sintered samples.

Sample	Parameters	(h k l)					a (Å)
		(1 1 1)	(2 0 0)	(2 2 0)	(3 1 1)	(2 2 2)	
0% CeO₂	2θ (°)	32.33	37.51	54.09	64.35	67.70	4.7978
	d (Å)	2.7681	2.3981	1.6960	1.4471	1.3853	
0.5 wt% CeO₂	2θ (°)	32.34	37.50	54.04	64.36	67.54	4.8232
	d (Å)	2.7661	2.3966	1.6961	1.4468	1.3854	
0.75 wt% CeO₂	2θ (°)	32.37	37.52	54.07	64.36	67.60	4.8223
	d (Å)	2.7630	2.3942	1.6953	1.4463	1.3850	
1 wt% CeO₂	2θ (°)	32.34	37.52	54.05	64.34	67.62	4.8161
	d (Å)	2.7655	2.3961	1.6960	1.4468	1.3852	

solid solution. In this study, the difference in radius between Ca^{2+} (0.099 nm) and Ce^{4+} (0.097 nm) was about 2.0%, but the difference in radius between Mg^{2+} (0.072 nm) and Ce^{4+} was nearly 26%. Therefore, CeO_2 is expected to dissolve easily in CaO but not in MgO, which is confirmed by the results of XRD analysis.

3.3. SEM Analysis.

Figure 3 shows the typical microstructure of the fracture surfaces of samples containing various amounts of CeO_2.

The sintered sample without CeO_2 addition has more pores and the grains in it were smaller in size compared with the samples with CeO_2 additions. Hence, adding CeO_2 increased the degree of sintering and densification and facilitated grain growth. MgO (dark gray) grains grew more rapidly than CaO (light gray) grains due to the fact that the periclase was the continuous phase surrounding lime and as such the growth of the isolated grains of CaO was hindered by the difficulty for Ca^{2+} to diffuse across the matrix during the sintering process. It can be seen that the number of pores decreased progressively as the CeO_2 content was increased to 0.75 wt%, but the number increased with further increase in CeO_2 content to 1 wt%, which is consistent with the results of Figure 1.
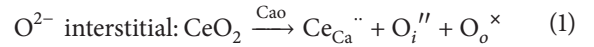
It can be also noted that pores were present at the boundaries between MgO and CaO grains or within the MgO grains; in all the samples no pores were observed within the CaO grains.

The number of pores at grain boundaries will decrease during the sintering process as a result of grain boundary migration, leading to the formation of bigger pores on crystal surface, which may be eliminated as the sintering process progresses. But with the introduction of CeO_2, the number and size of pores in the MgO grains gradually increased, as the amount of CeO_2 doping was increased. This cannot be attributed to the pore evolution in grains, but it may be due to the formation of Schottky lattice defects, which increased the oxygen vacancy concentration in the high-temperature sintering process. With the increasing of additions, the concentration of lattice defects increases and the vacancy formation energy decreases. As a consequence, the oxygen vacancies diffuse, accumulate, and condense to form pores in the grains in the crystal boundary-migration process [18]. Since the pores in the grains can only be eliminated by lattice

migration, which is much slower than the crystal boundary migration, it is difficult to eliminate the pores in MgO grains.

3.4. Effect of Defect Reaction by CeO_2 Doping.

CaO and MgO belong to the cubic system, as it is shown in Figure 4(a).

Figure 4(b) shows the crystal structure doped with CeO_2. When CeO_2 dissolved into CaO, as the valence of Ce^{4+} is higher than that of Ca^{2+} it may cause two kinds of defect reactions as follows:

$$O^{2-} \text{ interstitial: } CeO_2 \xrightarrow{Cao} Ce_{Ca}{}^{\cdot\cdot} + O_i{}'' + O_o{}^{\times} \quad (1)$$

$$Ca^{2+} \text{ vacancy: } CeO_2 \xrightarrow{Cao} Ce_{Ca}{}^{\cdot\cdot} + V_{Ca}{}'' + 2O_o{}^{\times} \quad (2)$$

Solid solution reactions in (1) and (2) comply with the law of conservation of mass and charge. The number of negative ions brought in by CeO_2 doping ($O^{2-} : Ce^{4+} = 2:1$) is more than that of CaO ($O^{2-} : Ca^{2+} = 1:1$) causing the surplus of negative ions and the shortage of positive ions. In order to maintain the electroneutrality, additional cation vacancy must be generated when Ce^{4+} dissolves in the CaO phase. Hence, Ca^{2+} vacancy in (2) is the prior modality of charge compensation while defects in MgO grains mainly come from heat-activation Schottky lattice defects as follows:

$$0 \rightleftharpoons V_{Mg}{}'' + V_O{}^{\cdot\cdot} \quad (3)$$

Generally, vacancies in the grains are surrounded by atoms, but atoms are not necessarily surrounded by vacancies. As a result, it is easy for vacancies to diffuse but it is difficult for atoms to diffuse. MgO-CaO materials doped with CeO_2 enlarge the vacancy concentration of Ca^{2+}. Owing to high symmetry of CaO crystal structure, the migration energy of Ca^{2+} vacancy is the same in the six neighboring directions (Figure 4(c)) and migration towards any direction may occur, which contributes to the Ca^{2+} diffusion. According to the defect reaction, prior modality of charge compensation in CaO lattice is the vacancy of positive ions, so, no pores occur in the sintering CaO grains while O^{2-} vacancy in MgO grains forms pores in grains.

4. Conclusions

(1) The lattice constant of CaO in MgO-CaO materials increases with the addition of CeO_2, when the amount
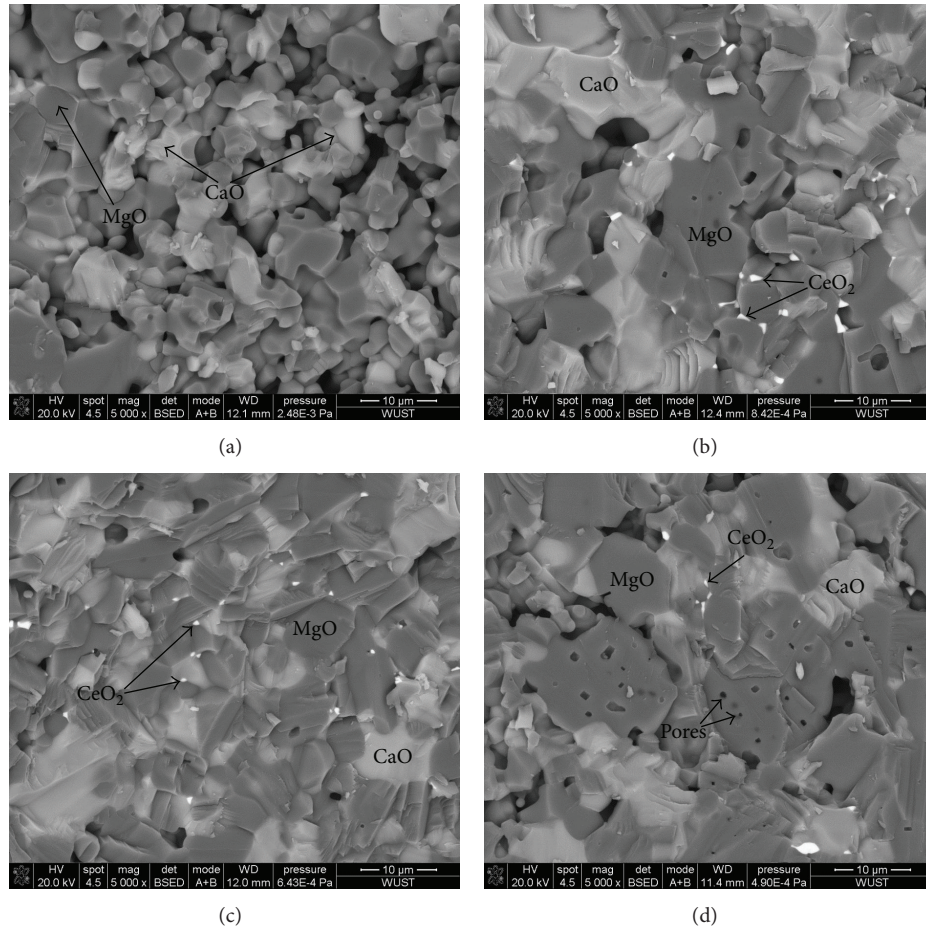
FIGURE 3: SEM images of samples: (a) 0%, (b) 0.5 wt%, (c) 0.75 wt%, and (d) 1 wt%.
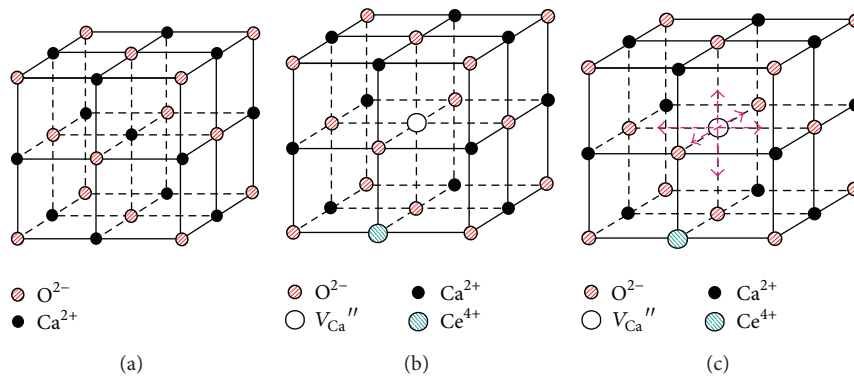

FIGURE 4: Schematic diagram for Crystal structure of CaO. (a) Crystal structure of CaO, (b) crystal structure of CaO doped with CeO_2, and (c) schematic diagram for vacancy migration of Ca^{2+}.

of addition exceeds 0.5 wt%, the lattice constant starts to decrease.

(2) The addition of CeO_2 increases the vacancy concentration of Ca^{2+} and accelerates the diffusion of Ca^{2+}, contributing to the sintering densification of materials. Many pores are formed in the grains of MgO, which mainly originated from the Schottky lattice defects and oxygen vacancy aggregation when the grain boundaries migrate during high-temperature sintering.

Acknowledgment

References

[1] W. E. Lee and R. E. Moore, "Evolution of in situ refractories in the 20th century," *Journal of the American Ceramic Society*, vol. 81, no. 6, pp. 1385–1410, 1998.

[2] Z. Q. Guo, S. Palco, and M. Rigaud, "Bonding of cement clinker onto doloma-based refractories," *Journal of the American Ceramic Society*, vol. 88, no. 6, pp. 1481–1487, 2005.

[3] Z. Li, S. Zhang, and W. E. Lee, "Improving the hydration resistance of lime-based refractory materials," *International Materials Reviews*, vol. 53, no. 1, pp. 1–20, 2008.

[4] M. Rabah and E. M. M. Ewais, "Multi-impregnating pitch-bonded Egyptian dolomite refractory brick for application in ladle furnaces," *Ceramics International*, vol. 35, no. 2, pp. 813–819, 2009.

[5] Y. W. Wei and N. Li, "Refractories for clean steel making," *American Ceramic Society Bulletin*, vol. 81, no. 5, pp. 32–35, 2002.

[6] X. Zhong, "Looking ahead-a new generation of high performance refractory ceramics," *Naihuo Cailiao*, vol. 37, no. 1, pp. 1–10, 2003.

[7] L. N. Zhong, B. L. Wu, J. G. Song et al., "Recycling refractory waste," *Journal of Functional Materials*, vol. 35, supplement, pp. 2615–2618, 2004.

[8] W. Meyer, A. Franchi, G. Buchebner, and M. Willingshofer, "The use of dolomite-carbon-lined ladles for the production of superclean steels," *Veitsch-Radex Rundschau*, vol. 1998, no. 2, pp. 32–44, 1998.

[9] N. M. Ghoneim, M. A. Mandour, and M. A. Serry, "Phase composition, microstructure and properties of sintered La_2O_3-doped lime and dolomite grains," *Ceramics International*, vol. 16, no. 4, pp. 215–223, 1990.

[10] A. Ghosh and H. S. Tripathi, "Sintering behaviour and hydration resistance of reactive dolomite," *Ceramics International*, vol. 38, no. 2, pp. 1315–1318, 2012.

[11] M. Chen, N. Wang, J. Yu, and A. Yamaguchi, "Effect of porosity on carbonation and hydration resistance of CaO materials," *Journal of the European Ceramic Society*, vol. 27, no. 4, pp. 1953–1959, 2007.

[12] A. Ghosh, T. K. Bhattacharya, B. Mukherjee, and S. K. Das, "Effect of CuO addition on the sintering of lime," *Ceramics International*, vol. 27, no. 2, pp. 201–204, 2001.

[13] H. A. Yeprem, "Effect of iron oxide addition on the hydration resistance and bulk density of doloma," *Journal of the European Ceramic Society*, vol. 27, no. 2-3, pp. 1651–1655, 2007.

[14] É. Makó, "The effect of quartz content on the mechanical activation of dolomite," *Journal of the European Ceramic Society*, vol. 27, no. 2-3, pp. 535–540, 2007.

[15] J. L. Rodríguez, M. A. Rodríguez, S. De Aza, and P. Pena, "Reaction sintering of zircon-dolomite mixtures," *Journal of the European Ceramic Society*, vol. 21, no. 3, pp. 343–354, 2001.

[16] J. Xue, J. H. Tinkler, and R. Dieckmann, "Influence of impurities on the oxygen activity-dependent variation of the oxygen content of a commercial, CaO-doped ZrO_2," *Solid State Ionics*, vol. 166, no. 1-2, pp. 199–205, 2004.

[17] M. Chen, C. Lu, and J. Yu, "Improvement in performance of MgO-CaO refractories by addition of nano-sized ZrO_2," *Journal of the European Ceramic Society*, vol. 27, no. 16, pp. 4633–4638, 2007.

[18] J.-K. Yan, G.-Y. Gan, J. Yuan, J.-H. Du, and J.-H. Yi, "Defect chemistry and formation mechanism of pores in undoped TiO_2 ceramics," *Chinese Journal of Nonferrous Metals*, vol. 21, no. 6, pp. 1380–1388, 2011.